# Complexation and Mechanism of Fluorescence Quenching of Telmisartan with Y(III) and Nd(III)

**Shaista Bano, Ayaz Mohd, Aftab Aslam Parwaz Khan, and K. S. Siddiqi***

Department of Chemistry, Aligarh Muslim University, Aligarh-202002, India

The determination of the stoichiometry of complex formation and the mechanism of fluorescence quenching of telmisartan (TMST) with Y(III) and Nd(III) was carried out in great detail by a fluorometric method. The quenching was interpreted in terms of chelation-enhanced quenching. The experimental results showed that both Y(III) and Nd(III) quench the intrinsic fluorescence of TMST without inducing any conformational change in it. The quenching of fluorescence was found to be static and due to the formation of a nonfluorescent complex in the ground state. Linear Stern−Volmer plots were obtained for both complexes. The pH of the solution was found to have a profound effect on quenching, and effective quenching was obtained at pH 7. The stoichiometry of metal−TMST complexes was found to be 1:2 through the Benesi−Hildebrand method. The quenching constant $K_{sv}$ and association constant were determined together with their thermodynamic parameters at (25, 35, and 45) °C. The negative $\Delta G$ values indicate that the complexation process is spontaneous. A decrease in log $K$ with an increase in temperature and the negative values of $\Delta H$ for the complexation show that all the complexation reactions are exothermic and the metal−ligand binding process is enthalpy driven.

## Introduction

Telmisartan (TMST), 4-[(2-*n*-propyl-4-methyl-6-(1-methylbenzimidazol-2-yl)benzimidazol-1-yl)methyl]biphenyl-2-carboxylic acid (Figure 1), is a known drug against high blood pressure (hypertension) which belongs to the group of angiotensin II receptor antagonists (ARA II).[1,2] TMST is highly selective for angiotensin II (AT1) receptors. It inhibits the angiotensin II receptor in a way that the effect of angiotensin II is blocked, resulting in a decrease of blood pressure.[3] The therapy these drugs offer is a good quality of life for hypertensive patients due to the absence of side effects and its once daily administration.[4] The key advantages of the nonpeptide ARA II antagonists are related to their specificity of action and minimization of untoward effects.[5] TMST is found to be effective in the suppression of murine experimental autoimmune uveoretinitis (EAU).[6] TMST undergoes minimal biotransformation in the liver to form TMST 1-*O*-acylglucuronide,[7] its major inactive metabolite. The maximum plasma concentration ($C_{max}$) occurs within about 3 h ($T_{max}$) after its oral administration, giving plasma levels of 50 $\mu g \cdot L^{-1}$ for a 40 mg dose. Renal excretion is a minor elimination pathway for TMST; hence, the dose excreted in urine is small (less than 1 %). The mean elimination half-life ($t_{1/2}$) is approximately 24 h, in contrast with the rapid absorption process of the drug. The rest of the parent compound (more than 98 %) is excreted in feces.[8] TMST has also been shown to form a double-helical metallocycle upon reaction with copper. Its catalytic properties toward the oxidative couple of 2,6-di-*tert*-butylphenol has also been investigated.[9]

In recent years, there has been an increased interest in the study of rare-earth complexes. Owing to the unique properties of the lanthanide ions, lanthanides have often been effectively employed as active Ca(II) and Mg(II) substitutes in many metalloproteins,[10] as chiral NMR shift reagents and MRI contrast agents,[11] and also as luminescent probes of metal binding in biological systems.[12] Rare-earth complexes have also been found to exhibit anticancer and fungicidal properties. The biological properties of the rare-earth ions, primarily based on their similarity to calcium, have been the basis for research into potential therapeutic applications since the early part of the 20th century.[13−17] While these rare-earth elements are being used in agriculture, medicine, and materials, they can be introduced into the environment and human bodies. To obtain information about the long-term effects of rare-earth elements on people, the complexes of lanthanide ions with amino acids as ligands have been synthesized and extensively studied by a variety of methods.[18]

The interaction of metal ions with drugs administered for therapeutic purposes is a subject of considerable interest.[19−22] It is known that some drugs work by chelation[19] or by inhibiting the formation of metalloenzymes.[20] Therefore, metal ions might play a vital role during the biological process of drug utilization in the body. The interaction of rare-earth ions and drugs can produce special antibacterial or anticancer effects.[22] It is well-known that the coordination ability of aromatic carboxylic acids toward rare-earth complexes has received considerable attention because of the strong coordination ability and varieties of bridging modes of the carboxylate group with regard to formation of extended frameworks.[23−25] TMST in its molecular structure has a carboxylate group which may provide a suitable site for rare-earth coordination. However, to the best of our knowledge, no research has been published concerning the interaction of rare-earth ions with TMST.

In this project, therefore, we have studied the interaction of TMST with Y(III) and Nd(III) through absorption and fluorescence spectroscopy. Fluorescence spectroscopy has been widely used to monitor the molecular interaction because of its high sensitivity, reproducibility, and relatively easy use. Such interac-

* Corresponding author. E-mail: ks_siddiqi@yahoo.co.in, aizi_pasha@yahoo.com.

10.1021/je100711u 
Published on Web 11/30/2010

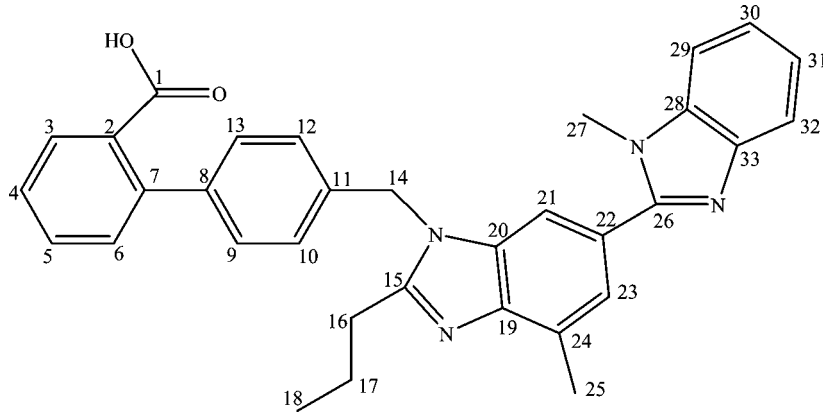


**Figure 1.** Structure of TMST.

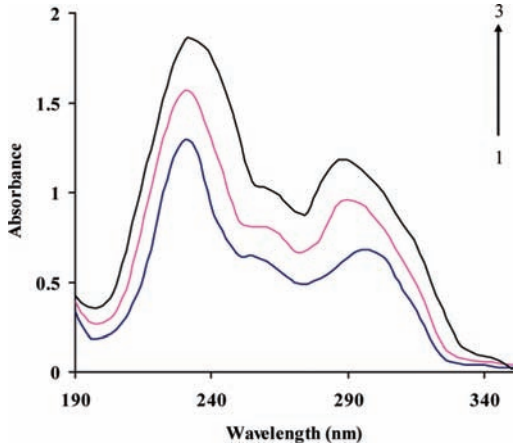


**Figure 2.** Absorption spectra of (1) TMST ($1 \cdot 10^{-4}$ M), (2) TMST−Y(III), and (3) TMST−Nd(III). The concentration of Y(III) and Nd(III) was $1 \cdot 10^{-3}$ M.

tions between TMST and these metal ions can cause fluorescence quenching. Therefore, valuable information such as the binding mechanism, association constant, and stoichiometry can be obtained using a fluorescence quenching study of TMST by these rare-earth ions. In addition, a thermodynamic study of the complexation behavior between these rare-earth ions and TMST was also done. Determination of the thermodynamic properties of the complexes can not only enrich the thermochemical database, but also help to understand some other physicochemical aspects of these complexes.

## Experimental Section

***Apparatus.*** The fluorescence emission spectra were scanned with a Hitachi-F-2500FL spectrophotometer. The absorption spectra were obtained with an Elico-SL-169 double-beam UV−vis spectrophotometer. All potentiometric measurements were done with an Elico-LI-120 pH meter.

***Materials and Methods.*** The concentration of the stock solution of TMST (Sigma-Aldrich), $1 \cdot 10^{-3}$ M, was prepared by dissolving it in 0.1 M NaOH and then diluting to a fixed volume with doubly distilled water. Solutions of Y(III) and Nd(III) (CDH Pvt. Ltd.), $2.0 \cdot 10^{-3}$ M, were prepared by dissolving $Y_2O_3$ and $Nd_2O_3$ (purity 99.99 %) in 1:1 HCl and evaporating the solution to almost dryness before diluting to 100 mL with water. The working standard solutions were prepared by making appropriate dilutions with doubly distilled water. Britton−Robinson (BR) buffer solutions of different pH values were prepared by mixing a mixed acid (composed of 0.04 M $H_3PO_4$, $CH_3COOH$, and $H_3BO_3$) with 0.2 M NaOH proportionately. The pH values were measured with a pH meter and adjusted accordingly. All reagents were of analytical reagent grade, and doubly distilled water was used throughout.

Appropriate amounts of TMST ($1 \cdot 10^{-5}$ M) and different amounts of metal chloride solutions were transferred to 10 mL flasks to give a final concentration between ($0.5 \cdot 10^{-6}$ and $1.5 \cdot 10^{-4}$) M. After the addition of 1 mL of BR buffer (pH 7.0), the solution was made up to volume with distilled water. The steady-state fluorescence spectra of TMST alone and after the addition of different amounts of Y(III) and Nd(III) were recorded in the $\lambda_{em}$ = (320 to 550) nm region at $\lambda_{ex}$ = 300 nm. The synchronous fluorescence spectra were scanned at $\Delta\lambda = 65$ nm ($\Delta\lambda = \lambda_{em} - \lambda_{ex}$). The absorption spectra of TMST ($1 \cdot 10^{-4}$ M) alone and in the presence of Y(III) and Nd(III) ($1 \cdot 10^{-3}$ M) were scanned in the (190 to 350) nm region.

## Results and Discussion

***Absorption Spectra.*** The absorption spectrum of TMST ($1 \cdot 10^{-4}$ M) shows a strong peak at 230 nm and another one at 295 nm (Figure 2) corresponding to two chromophores. When Y(III) and Nd(III) were added to it, the peak at 295 nm moved to a shorter wavelength with an increase in intensity, although the position of the peak at 230 nm did not change. The p$K_a$ of TMST (4.45) corresponds to the acid−base equilibrium in which the carboxylic group is involved.[26] Its deprotonation will, therefore, occur at pH 7, and TMST will exist as an anion. Its complexes with trivalent metal ions will mainly be formed by ion−dipole interaction because any significant absorption band due to orbital−orbital interaction is not observed. The increase of absorption bands present in the spectrum of TMST due to addition of Y(III) and Nd(III) clearly indicates that TMST is complexed by Y(III) and Nd(III).

***Fluorescence Emission Spectra.*** TMST contains two fluorophores, biphenyl and benzimidazole,[27,28] which exhibit strong fluorescence in basic media.[26] When excited at 300 nm at pH 7, the maximum fluorescence was observed at 365 nm. When different amounts of Y(III) and Nd(III) were titrated against a fixed concentration of TMST, its fluorescence intensity decreased regularly without any change in $\lambda_{em}$ (Figure 3), which indicates that both Y(III) and Nd(III) quench the intrinsic fluorescence. Fluorescence quenching is the decrease of the quantum yield of fluorescence from a fluorophore induced by a variety of molecular interactions, such as excited-state reactions, photoinduced electron transfer (PET), fluorescence resonance energy transfer, ground-state complex formation, and collisional quenching.[29] The physical origin of fluorescence quenching arising from the addition of a quenching agent, Y(III) and Nd(III), to the TMST fluorescence can be interpreted in terms

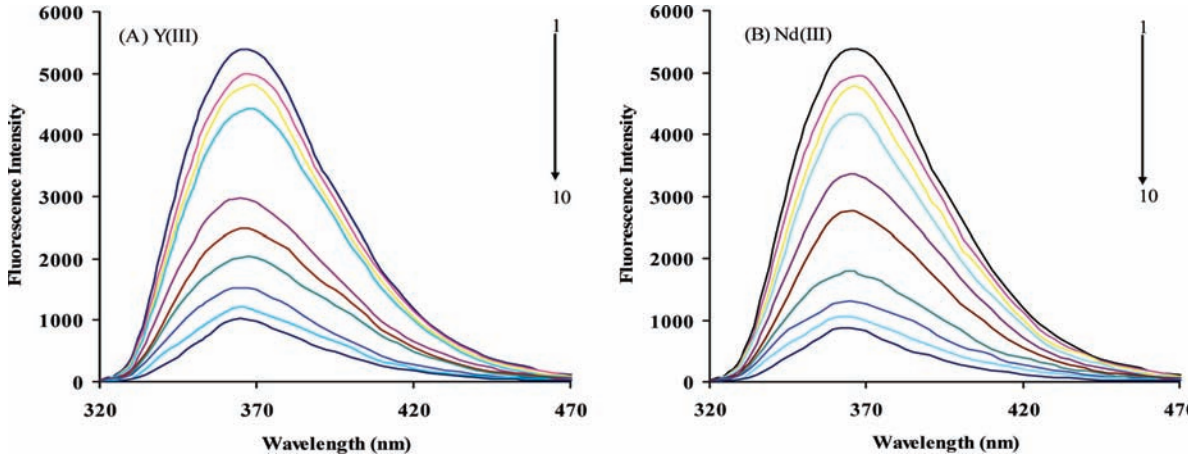


**Figure 3.** Fluorescence emission spectra ($\lambda_{ex}$ = 300 nm) of TMST with Y(III) (A) and Nd(III) (B) at 25 °C: 1, $1 \cdot 10^{-5}$ M TMST; 2 to 9, addition of (0.5, 1, 5, 10, 30, 60, 90,120, and 150) $\mu$M metal ions.

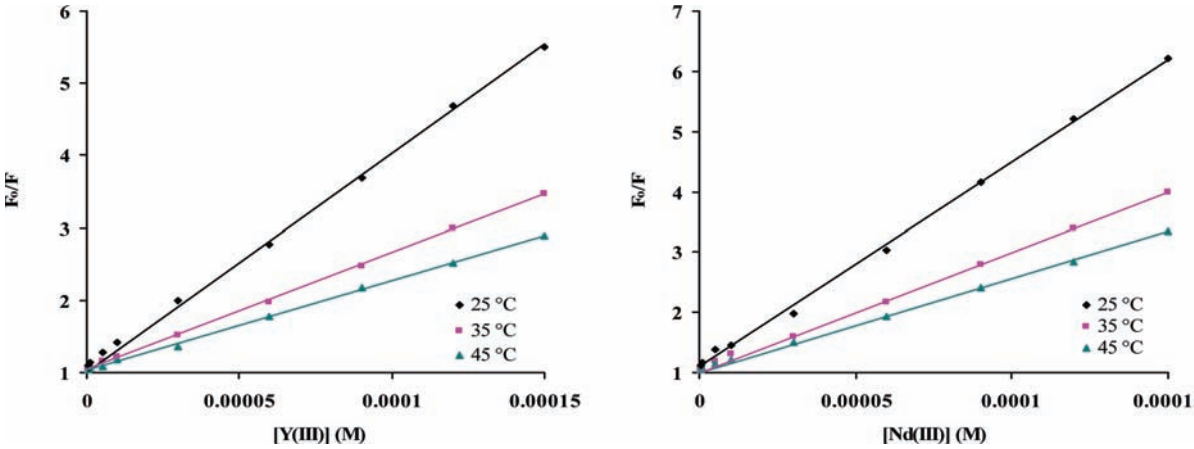


**Figure 4.** Stern−Volmer plot of TMST with Y(III) and Nd(II) at (25, 35, and 45) °C.

of chelation-enhanced fluorescence quenching (CHEQ). In CHEQ the fluorophore itself (TMST) is fluorescent when the receptor site (carboxylic group) is free. In the presence of metal ions, the fluorescence intensity is lowered due to chelation of the metal ion to the receptor unit of the sensor and formation of a nonfluorescent complex, and therefore, the net fluorescence is quenched. Basically, this quenching process can be divided into two kinds of mechanisms: static and dynamic quenching. Static and dynamic quenching can be distinguished by their different dependences on the temperature and excited-state lifetime. Dynamic quenching is diffusion controlled because the quencher must diffuse to the fluorophore during the lifetime of the excited state. Since high temperature will result in a large diffusion coefficient, the bimolecular quenching constants are expected to increase with temperature. If $K_{sv}$ decreases with increasing temperature, it may be concluded that the quenching process is static rather than dynamic.[30−32] Static quenching implies either the existence of a sphere of effective quenching or the formation of a ground-state nonfluorescent complex, whereas collisional or dynamic quenching involves the collision followed by the formation of a transient complex between an excited-state fluorophore and a ground-state quencher. The excited-state complex dissociates upon radiative and nonradiative deactivation. Quenching can also occur via many trivial processes, such as attenuation of the excitation light by the fluorophore itself or other absorbing species. Except for trivial processes, the quenching mechanisms involve very close contact between the excited state of a fluorescent species and the quencher and are sometimes referred to as contact quenchers. The quenching can be mathematically expressed by the Stern−Volmer equation, which allows the quenching constant to be calculated:[33,34]

$$F_o/F = 1 + K_q \cdot \tau_o[Q] = 1 + K_{sv}[Q] \quad (1)$$

Here $F_o$ and $F$ are the fluorescence intensities in the absence and presence of the quencher, respectively, $K_q$ is the bimolecular quenching rate constant, $\tau_o$ is the average lifetime of the molecule without quencher, [Q] is the concentration of the quencher, and $K_{sv}$ is the Stern−Volmer quenching constant. In the presence of a quencher, Y(III) and Nd(III), the fluorescence intensity is reduced from $F_o$ to $F$. The ratio $F_o/F$ is directly proportional to the quencher concentration [Q].

Evidently

$$K_{sv} = K_q \cdot \tau_o \quad (2)$$

$$F_o/F = 1 + K_{sv}[Q] \quad (3)$$

According to eq 3, a plot of $F_o/F$ versus [Q] shows a linear graph with an intercept of 1 and a slope of $K_{sv}$.[35] Figure 4 displays the Stern−Volmer plots of quenching of TMST by Y(III) and Nd(III) ions at three different temperatures [(25, 35, and 45) °C]. The resulting regression equations for these ions are summarized in Table 1. The results show that $K_{sv}$ is inversely correlated with the temperature, which indicates that the

**Table 1. Stern−Volmer Constants at (25, 35, and 45) °C**

| | $K_{sv}$ | | | | | |
|---|---|---|---|---|---|---|
| | L·mol$^{-1}$ | | | *R* | | |
| metal ion | 25 °C | 35 °C | 45 °C | 25 °C | 35 °C | 45 °C |
| Y(III) | 30251 | 16551 | 12994 | 0.9986 | 0.9991 | 0.9979 |
| Nd(III) | 34798 | 19882 | 15588 | 0.9984 | 0.9985 | 0.9978 |

probable quenching mechanism is not initiated by dynamic quenching but by complex formation.[36]

It is also possible to distinguish between these two mechanisms of quenching by simple examination of the absorption spectra of the system under study. Since collisional quenching affects only the excited state of the fluorophore, there are typically no changes in the fluorophore absorption spectra, whereas ground-state complex formation and subsequent static quenching frequently result in marked changes in the absorption spectrum. Figure 2 shows that the absorption peak of TMST at 295 nm is blue-shifted with an increase in absorption intensity upon addition of Y(III) and Nd(III), which suggests that the interaction of TMST with these metal ions is mainly a static quenching process.

The emission spectra of TMST show that in the presence of Y(III) and Nd(III) the fluorescence is quenched but there is no shift in the emission position, which indicates that the metal ions quench the intrinsic fluorescence of TMST without inducing any conformational change, and the absence of any new emission band upon complexation excludes the possibility of formation of an exciplex. The conformational changes were further confirmed by synchronous spectra. Figure 5 shows the synchronous spectra of TMST with Y(III) and Nd(III) at $\Delta\lambda$ = 65 nm. The spectra clearly show that the emission wavelength kept its position in the investigated concentration range. Therefore, fluorescence quenching due to formation of an exciplex (excited-state complex) is excluded. The exciplex formation quenching is a process which competes with emission for depopulation of the excited state; thus, the fluorescence decreases in proportion to the yield. Another important quenching process, which has been used to describe quenching mechanisms, is fluorescence resonance energy transfer (FRET).[37] FRET is the transfer of the excited-state energy from the initially excited TMST, L*, to a complex, ML, which is typically nonfluorescent. As shown in Figure 6 the L* emission spectrum did not significantly overlap with the absorption spectrum of ML; therefore, the possibility of FRET is also precluded.

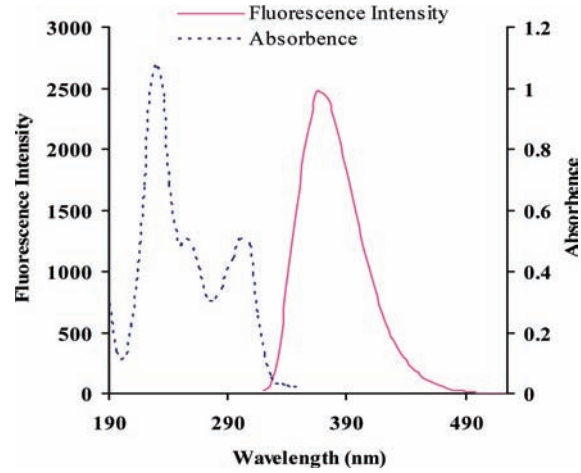


**Figure 6.** Comparison between absorption and fluorescence emission spectra.

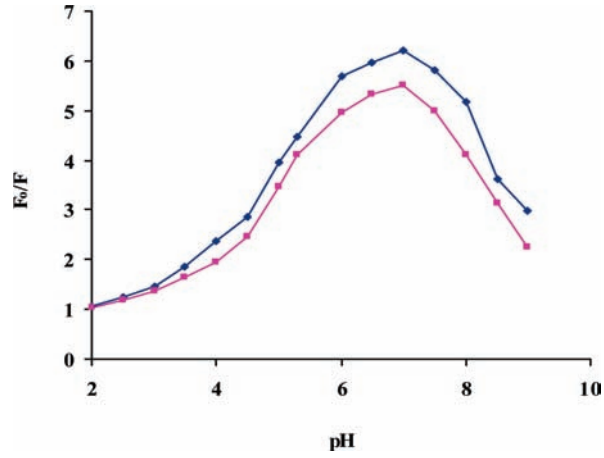


**Figure 7.** Effect of the pH on the quenching factor ($F_o/F$) with Y(III) and Nd(III).

***Effect of the pH on Complexation.*** The experimental results (Figure 7) indicate that the quenching factor ($F_o/F$) increases steadily up to pH 7 and suddenly falls above this pH. These results can be explained as follows: Y(III) and Nd(III) might coordinate with the carboxyl groups of TMST. Obviously, it is disadvantageous to coordinate TMST with the Y(III) and Nd(III) ions in the acidic environment. Also, Y(III) and Nd(III) will be

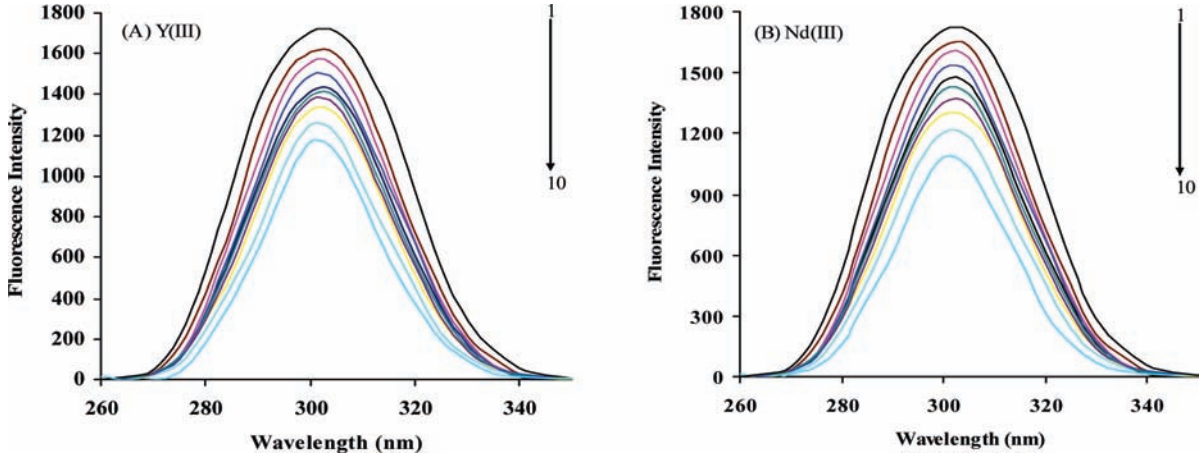


**Figure 5.** Synchronous spectra ($\Delta\lambda$ = 65 nm) of TMST with Y(III) (A) and Nd(III) (B) at 25 °C: 1, 1·10$^{-5}$ M TMST; 2 to 9, addition of (0.5, 1, 5, 10, 30, 60, 90, 120, and 150) $\mu$M metal ions.

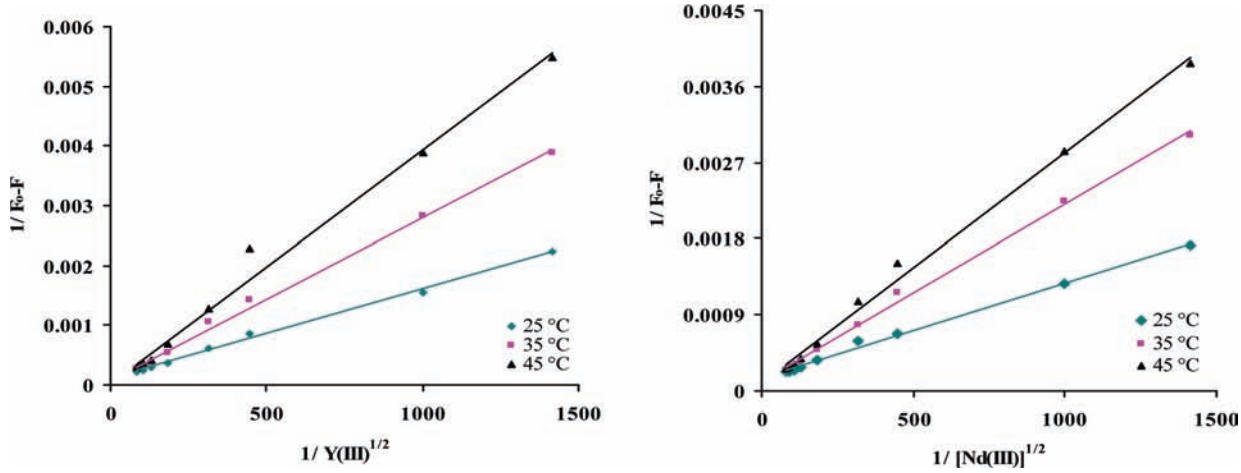


**Figure 8.** Double-reciprocal plots of TMST with Y(III) and Nd(II) at (25, 35, and 45) °C.

precipitated in a strong alkaline medium, which will block the coordination between TMST and the metal ions. Since the change in pH influences the stability of the fluorescent complexes and results in changes in the fluorescence character, selection of the pH is important, and pH 7.0 was therefore selected for further research.

The experiments indicate that the buffers also have a large effect on the fluorescence intensity of the system. Some buffers were tested as follows: $CH_3COOH-NaOOCCH_3$, borax−HCl, $NaHPO_4$−HCl, $KH_2PO_4$−NaOH, phthalate−NaOH, and BR. Of all buffers examined, BR appears to be the most effective and useful (pH 7).

***Stoichiometry and Association Constant.*** The association constant of the complexes was determined by the Benesi−Hildebrand method using fluorescence quenching data.[38,39] The Benesi−Hildebrand plots were examined to characterize further the stoichiometry of the metal−TMSTcomplexes.

In the case of a 1:1 complex, the following equation is applicable:

$$1/F_o - F = 1/(F_o - F_\infty)K[\mathrm{Me}]_o + 1/(F_o - F_\infty) \quad (4)$$

In this approach, a graph of $1/(F_o - F)$ versus $1/[\mathrm{Me}]_o$ was made. $F$ is the observed fluorescence at each concentration tested, $F_o$ is the fluorescence intensity of the analyte in the absence of metal ion, $F_\infty$ is the fluorescence intensity at saturation, and $[\mathrm{Me}]_o$ is the concentration of the metal ion. A linear plot is required for this double-reciprocal plot to conclude 1:1 stoichiometry.

In the case where 1:2 stoichiometry is predominant, the applicable equation is

$$1/F_o - F = 1/(F_o - F_\infty)K[\mathrm{Me}]_o^{1/2} + 1/(F_o - F_\infty) \quad (5)$$

For a 1:2 complex, a straight line will be obtained when $1/(F_o - F)$ is plotted against $1/[\mathrm{Me}]_o^{1/2}$.

The data when fitted according to the Benesi−Hildebrand plot assuming 1:2 stoichiometry (eq 5) give a straight line, while a downward concave curvature is obtained when the data are fitted assuming 1:1 stoichiometry using eq 4. It is therefore concluded that in all cases the stoichiometry of the formed complexes between rare-earth ions and TMST is 1:2. Figure 8 shows the double-reciprocal curve, and Table 2 gives the corresponding calculated results. The linear correlation coefficients for all the curves are larger than 0.996, indicating that the interaction between metal ions and TMST agrees well with the site-binding model underlying eq 5.

**Table 2. Binding Constants and Regression Coefficients at (25, 35, and 45) °C**

| | log $K$ | | | $R$ | | |
|---|---|---|---|---|---|---|
| metal ion | 25 °C | 35 °C | 45 °C | 25 °C | 35 °C | 45 °C |
| Y(III) | 2.00 | 1.367 | 0.8751 | 0.9983 | 0.9983 | 0.9964 |
| Nd(III) | 2.301 | 1.699 | 1.222 | 0.9977 | 0.9986 | 0.9969 |

There are two coordinating sites in PUFX, nitrogen and oxygen. The oxygen atom tends to form a stable complex with a rare-earth element, due to its strong affinity for Y(III) and Nd(II). On the other hand, the stability of the complex formed with a rare-earth element by a nitrogen atom is relatively poor. Usually, oxygen atoms in an organic ligand coordinate with the rare-earth element in two ways: the negatively charged oxygen forms a stable ionic bond, while neutral oxygen forms a coordinate bond.[40] On the basis of the above discussion, a structure of the formed complex has been proposed. Since the estimated $pK_a$ value of TMST is about 4.5,[26] the deprotonation probably occurs at the carboxylic group of TMST in the solution (pH 7), which strongly supports the hypothetical structure proposed in Figure 9.

***Thermodynamic Parameters and Nature of the Binding Forces.*** Considering the dependence of the binding constant on the temperature, a thermodynamic process was considered to be responsible for this interaction. The thermodynamic parameters, enthalpy ($\Delta H$), entropy ($\Delta S$), and Gibbs energy ($\Delta G$), are the main evidence to determine the binding mode. For the purpose of clarifying the interaction between TMST and Y(III) and Nd(III), we carried out binding studies at three different temperatures: (25, 35, and 45) °C. $\Delta G$ can be estimated from the following equation, based on the binding constant at different temperatures:

$$\Delta G = -2.303RT \log K \quad (6)$$

where $R$ is the gas constant, $T$ is the temperature, and $K$ is the binding constant. From the value of the stability constant at different temperatures the enthalpy can be calculated by using eq 7. If the enthalpy ($\Delta H$) does not vary significantly over the

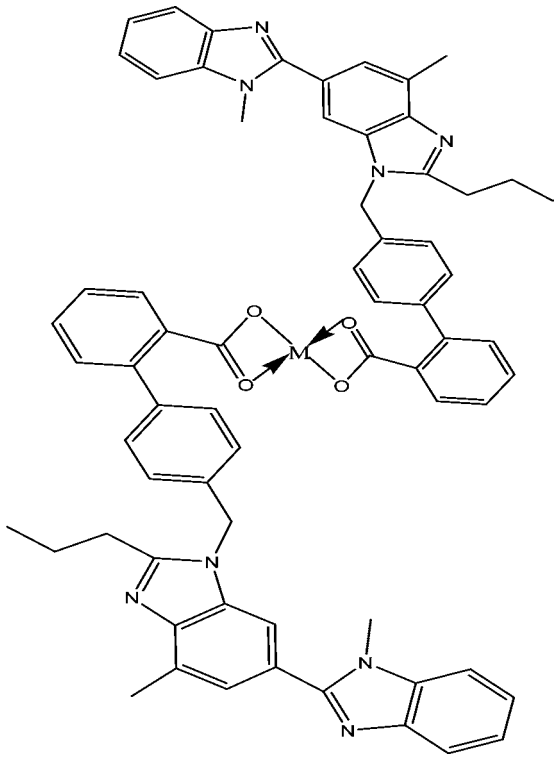

**Figure 9.** Proposed structure of the TMST complex (M = Y(III), Nd(III)).

**Table 3. Thermodynamic Parameters at (25, 35, and 45) °C**

| | $\Delta G$ | | | | |
|---|---|---|---|---|---|
| | kJ·mol$^{-1}$ | | | $\Delta H$ | $\Delta S$ |
| metal ion | 25 °C | 35 °C | 45 °C | kJ·mol$^{-1}$ | J·mol$^{-1}$·K$^{-1}$ |
| Y(III) | −11.411 | −8.067 | −5.328 | −102.157 | −304.841 |
| Nd(III) | −13.129 | −10.019 | −7.439 | −97.995 | −285.062 |

studied temperature range, then it can be regarded as a constant, and its value can be obtained from the van't Hoff equation.

$$\log K = -\Delta H/2.303RT + \Delta S/2.303R \quad (7)$$

The enthalpy ($\Delta H$) for the complexation process was evaluated from the slope of the plot of log $K$ vs $1/T$ using the graphical representation of van't Hoff's equation, and the entropy ($\Delta S$) could then be calculated using eqs 8 and 9.

$$\Delta G = \Delta H - T\Delta S \quad (8)$$

$$\Delta S = (\Delta H - \Delta G)/T \quad (9)$$

The calculated thermodynamic parameters for the complexation of TMST−Y(III) and TMST−Nd(III) are included in Table 3. It is observed from the tables that all the values of the thermodynamic parameters are negative. The negative $\Delta G$ values indicate that the complexation process is spontaneous. A decrease in log $K$ with an increase in temperature and the negative values of $\Delta H$ for the complexation show that all the complexation reactions are exothermic and the metal−ligand binding process is enthalpy driven. However, the $\Delta S$ values are all negative, and the complexation has an unfavorable change of entropy. The low numerical values of the stability constant suggest that the metal complexes are soluble in water and can readily dissociate into the metal ionic form. Generally, metal−ligand complexes with stability constants of 3 and lower are substantially (over ~5 %) ionized at the physiological pH of 7.4.

## Conclusions

We have investigated the interaction of TMST with Y(III) and Nd(III) by spectroscopic methods, including fluorescence quenching spectra and UV−vis absorption spectra. The experimental results indicate that the intrinsic fluorescence of TMST is quenched through a static quenching mechanism. A 1:2 (metal:drug) complex is formed. The stoichiometry and association constants log $K$ were evaluated according to the Benesi−Hildebrand method. The negative values of the thermodynamic parameters ($\Delta G$, $\Delta H$, and $\Delta S$) indicate that the complexation process is spontaneous, exothermic, and entropically unfavorable.

## Literature Cited


(1) Pitt, B.; Konstam, M. A. Overview of Angiotensin II-Receptor Antagonists. *Am. J. Cardiol.* **1998**, *82*, 47S–49S.
(2) Unger, T. Significance of Angiotensin type 1 Receptor Blockade: Why are Angiotensin II Receptor Blockers Different? *Am. J. Cardiol.* **1999**, *84*, 9S–15S.
(3) Willenheimer, R.; Dahlof, B.; Rydberg, E.; Erhardt, L. $AT_1$-Receptor Blockers in Hypertension and Heart Failure: Clinical Experience and Future Directions. *Eur. Heart J.* **1999**, *20*, 997–1008.
(4) Velasquez, M. T. Angiotensin II Receptor Blockers: A New Class of Antihypertensive Drugs. *Arch. Fam. Med.* **1996**, *5*, 351–356.
(5) Eberhardt, R. T.; Kevak, R. M.; Kang, P. M.; Frishman, W. H. Angiotensin II Receptor Blockade: An Innovative Approach to Cardiovascular Pharmacotherapy. *J. Clin. Pharmacol.* **1993**, *33*, 1023–1038.
(6) Okunuki, Y.; Usui, Y.; Nagai, N.; Kezuka, T.; Ishida, S.; Takeuchi, M.; Goto, H. Suppression of Experimental Autoimmune Uveitis by Angiotensin II Type 1 Receptor Blocker Telmisartan. *Invest. Ophthalmol. Visual Sci.* **2009**, *50*, 2255–2261.
(7) Ebner, T.; Heinzel, G.; Prox, A.; Beschke, K.; Wachsmuth, H. Disposition and Chemical Stability of Telmisartan 1-*O*-Acylglucuronide. *Drug Metab. Dispos.* **1999**, *27*, 1143-/1149.
(8) McClellan, K. J.; Markham, A. Telmisartan. *Drugs* **1998**, *56*, 1039-/1044.
(9) Zhao, J.; Mi, L.; Hu, J.; Hou, H.; Fan, Y. Cation Exchange Induced Tunable Properties of a Nanoporous Octanuclear Cu(II) Wheel with Double-Helical Structure. *J. Am. Chem. Soc.* **2008**, *130*, 15222–15223.
(10) Hughes, M. N. *The Inorganic Chemistry of Biological Processes*; Wiley: New York, 1975.
(11) Yam, V. W.-W.; Lo, K. K.-W. Recent Advances in Utilization of Transition Metal Complexes and Lanthanides as Diagnostic Tools. *Coord. Chem. Rev.* **1999**, *184*, 157–240.
(12) Bunzli, J. C. G. In *Lanthanide Probes in Life, Chemical and Earth Sciences*; Bunzli, J. C. G., Choppin, G. R., Eds.; Elsevier: Amsterdam, 1989; Chapter 7, p 219.
(13) Sharma, R. C.; Thripathi, S. P.; Kanna, K. S.; Sharma, R. S. Biologically Active Mixed-Ligand Complexes of Rare Earths. *Curr. Sci.* **1981**, *50*, 748–750.
(14) Evans, C. H. Interesting and Useful Biochemical Properties of Lanthanides. *Trends Biochem. Sci.* **1983**, *8*, 445–449.
(15) Zhang, J. C.; Xu, S. J.; Wang, K.; Yu, S. F. Effects of the Rare Earth Ions on Bone Resorbing Function of Rabbit Mature Osteoclasts in Vitro. *Chin. Sci. Bull.* **2003**, *48*, 2170–2175.
(16) Fricker, S. P. The Therapeutic Application of Lanthanides. *Chem. Soc. Rev.* **2006**, *35*, 524–533.
(17) Yumnam, S.; Rajkumari, L. Thermodynamics of the Complexation of *N*-(Pyridin-2-ylmethylene) Isonicotinohydrazide with Lighter Lanthanides. *J. Chem. Eng. Data* **2009**, *54*, 28–34.
(18) Zhang, J. N.; Tan, Z. C.; Liu, B. P.; Shi, Q.; Tong, B. Thermochemical Behavior of Crystalline RE(Val)$Cl_3$·$6H_2O$ (RE = Nd, Er, Val = Valine). *J. Chem. Eng. Data* **2009**, *54*, 392–395.
(19) Albert, A. *The Physico-Chemical Basis of Therapy: Selective Toxicity*, 6th ed.; Chapman and Hall: London, 1979.
(20) Hughes, M. N. *The Inorganic Chemistry of Biological Processes*, 2nd ed.; Wiley: New York, 1981.
(21) Liu, J.; Wang, E. B.; Peng, J.; Zhou, Y. S. Anti-Influenza Virus Activity of Heteropoly Complexes Containing Rare Earth Elements. *J. Rare Earths* **1999**, *17*, 139–142.
(22) Khalil, M. M.; El-Deeb, M. M.; Mahmoud, R. K. Equilibrium Studies of Binary Systems Involving Lanthanide and Actinide Metal Ions and

Some Selected Aliphatic and Aromatic Monohydroxamic Acids. *J. Chem. Eng. Data* **2007**, *52*, 1571–157.
(23) Li, Y.; Zheng, F. K.; Liu, X.; Zou, W. Q.; Guo, G. C.; Lu, C. Z.; Huang, J. S. Crystal Structures and Magnetic and Luminescent Properties of a Series of Homodinuclear Lanthanide Complexes with 4-Cyanobenzoic Ligand. *Inorg. Chem.* **2006**, *45*, 6308–6316.
(24) Azab, H. A.; El-Korashy, S. A.; Anwar, Z. M.; Hussein, B. H. M.; Khairy, G. M. Eu(III)−Anthracene-9-carboxylic Acid as a Responsive Luminescent Bioprobe and Its Electroanalytical Interactions with *N*-Acetyl Amino Acids, Nucleotides, and DNA. *J. Chem. Eng. Data* **2010**, *55*, 3130–3141.
(25) Li, H.; Xian, H.; Zhao, G. Synthesis and Crystal Structure of La(III), Y(III) Complexes of Homoveratic Acid with 1,10-Phenanthroline. *J. Rare Earths* **2010**, *28*, 7–11.
(26) Cagigal, E.; Gonzalez, L.; Alonso, R. M.; Jimenez, R. M. p$K_a$ Determination of Angiotensin II Receptor Antagonists (ARA II) by Spectrofluorimetry. *J. Pharm. Biomed. Anal.* **2001**, *26*, 477–486.
(27) Katritzky, A. R.; Rees, C. W. *Comprehensive Heterocyclic Chemistry: The Structure, Reactions, Synthesis and Uses of Heterocyclic Compounds*; Pergamon Press: London, 1984.
(28) Verdasco, G.; Martín, M. A.; del Castillo, B.; López-Alvarado, P.; Menéndez, C. Solvent Effects on the Fluorescent Emission of Some New Benzimidazole Derivatives. *Anal. Chim. Acta* **1995**, *303*, 73–78.
(29) Bhattacharyya, M.; Chaudhuri, U.; Poddar, R. K. Evidence for Cooperative Binding of CPZ with Hemoglobin. *Biochem. Biophys. Res. Commun.* **1990**, *167*, 1146–1153.
(30) Guo, M.; Zou, J. W.; Yi, P. G.; Shang, Z. C.; Hu, G. X.; Yu, Q. S. Binding Interaction of Gatifloxacin with Bovine Serum Albumin. *Anal. Sci.* **2004**, *20*, 465–470.
(31) Wang, C.; Wu, Q. H.; Li, C. R.; Wang, Z.; Ma, J. J.; Zang, X. H.; Qin, N. X. Interaction of Tetrandrine with Human Serum Albumin: A Fluorescence Quenching Study. *Anal. Sci.* **2007**, *23*, 429–433.
(32) Siddiqi, K. S.; Bano, S.; Mohd, A.; Khan, A. A. P. Binding Interaction of Captopril with Metal Ions: A Fluorescence Quenching Study. *Chin. J. Chem.* **2009**, *27*, 1755–1761.
(33) De Costa, M. D. P.; Jayasinghe, W. A. P. A. Detailed Studies on Complexation Behaviour and Mechanism of Fluorescence Quenching of Naphthalene Linked Hydroxamic Acid with Transition Metal Ions by UV−Visible and Fluorescence Spectra. *J. Photochem. Photobiol.* **2004**, *162*, 591–598.
(34) Stern, O.; Volmer, M. The Extinction Period of Fluorescence. *Phys. Z.* **1919**, *20*, 183–188.
(35) Hadjmohamadia, M. R.; Chaichi, M. J.; Biparva, P.; Alizadeh, K. Determination of Aliphatic Amines Using Fluorescence Intensity of 4-Methyl Umbelliferone. *Spectrochim. Acta, A* **2008**, *70*, 358–361.
(36) Lakowicz, J. R. *Principles of Fluorescence Spectroscopy*, 2nd ed.; Plenum: New York, 1999; pp 237−265.
(37) Bordbar, M.; Shamsipur, M.; Alizadeh, N. Thermodynamics Studies of Fluorescence Quenching and Complexation Behavior of Thallium(I) Ion with Some Polyazamacrocycles. *J. Photochem. Photobiol., A* **2006**, *178*, 83–89.
(38) Benesi, H.; Hildebrand, J. H. A Spectrophotometric Investigation of the Interaction of Iodine with Aromatic Hydrocarbons. *J. Am. Chem. Soc.* **1949**, *71*, 2703–2707.
(39) Jisha, V. S.; Thomas, A. J.; Ramaiah, D. Fluorescence Ratiometric Selective Recognition of $Cu^{2+}$ Ions by Dansyl−Naphthalimide Dyads. *J. Org. Chem.* **2009**, *74*, 6667–6673.
(40) Jiang, Z.; Cai, R.; Zhang, H. *Analytical Chemistry of Rare Earths*, 2nd ed.; Science Publishing: Beijing, 2000; pp 21−30.

Received for review July 3, 2010. Accepted November 6, 2010.

JE100711U